Title

Investigating the Co-occurance of Extreme Heat and Dust at California’s Salton Sea

Author
Stevens, Michael

Publication Date
2026

Investigating the Co-occurance of Extreme Heat and Dust at California's Salton Sea

Michael Stevens

Spring 2026

Professor Alexandra Heaney

12 June, 2026

[redacted]

Introduction:

Background:

Climate change has significantly increased the frequency of extreme heat and dry events throughout the world (Zhang et al., 2022). Regions like the Sahara, Northeast America, and Central Asia have seen the greatest uptick in the number of these events coinciding with one another (Zhang et al., 2022). This has profound implications for the long term health of drying saline lake ecosystems throughout the world. The compound exposure of extreme heat and dust around these ecosystems as they recede poses notable hazards for public health, particularly for disadvantaged communities. The co-exposure of these two environmental hazards creates a synergistic effect, where the cumulative hazard posed is significantly greater than the sum of the individual components (Rahman et al., 2022). Compound heat and dust exposure has been linked to increased systemic inflammation, oxidative stress, and impaired thermoregulation in affected subjects, overworking the heart and lungs (Rahman et al., 2022). Investigating compound extreme heat and dust events and the subsequent health outcomes of these events, particularly through the lens of health equity, is thus crucial for climate adaptation and ensuring environmental justice moving forward.

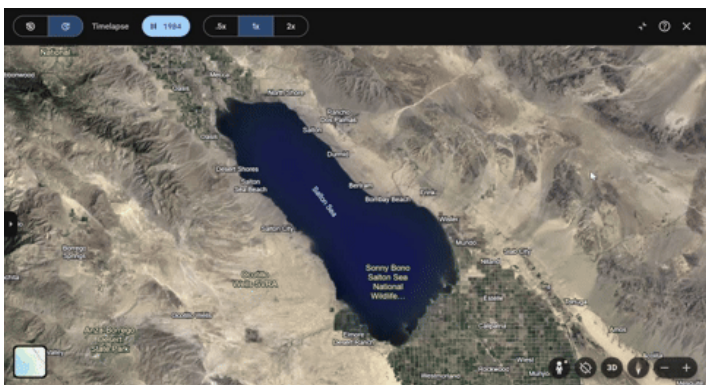

Figure 1. Google Earth Engine satellite imaging time-lapse of the Salton Sea's recession from 1984 to 2022.

A relevant example of climate and policy-driven compound exposure around these drying saline lake ecosystems is California's Salton Sea. An artificially-created saline lake in Imperial and Riverside counties, the Salton Sea was originally formed in 1905, when a routing accident as the Colorado River was being diverted into the Imperial Valley resulted in the Salton Basin filling with water over the next 2 years before repairs could be completed (Cantor & Knuth, 2018). Agricultural runoff from the surrounding Imperial Valley agricultural industry sustained the Sea's extent after its formation, defying predictions that the new artificial lake would soon evaporate and recede (Cantor & Knuth, 2018). This eventually resulted in a boom in tourism in the 1950s and 60s in the area, with booming resort towns like Bombay Beach on the west end of the Sea seen as potentially becoming the next Palm Springs (Cantor & Knuth, 2018). However, over the next couple decades pollution from the farm runoff that had been sustaining the Salton Sea's extent gradually degraded the lake's water quality. This resulted in mass fish die offs via eutrophication, where a surge in plant life growth (such as algal blooms) from excess nitrogen and phosphorus nutrients results in diminished oxygen levels upon their decay (Upadhyay et al., 2013). By the dawn of the 1980s, the Salton Sea had deteriorated in water quality substantially, resulting in mass ecosystem collapse and a subsequent flight of tourism that left the area as a ghost town (Cantor & Knuth, 2018). The remaining communities in the area today have substantially lower median annual household incomes and higher rates of respiratory issues like asthma than California state averages (SimplyAnalytics Staff, 2026). More recently, the Quantification Settlement Agreement (QSA) of 2003 engineered the largest agriculture-to-urban freshwater transfer in U.S. history, diverting Colorado River water from the Imperial Irrigation District to the San Diego County Water Authority in order to support its growing communities (Freund et al., 2022). This, combined with historic droughts, the long term decline of the Colorado River, and more water-efficient agricultural practices, has greatly reduced runoff inflow to the Salton Sea (Freund et al., 2022). Figure 1 shows a satellite imaging time-lapse of the Salton Sea's extent from 1984 to 2022 in Google Earth Engine, and demonstrates a significant uptick in the pace of the Sea's shrinkage after the 2003 QSA.

This accelerated recession of the Salton Sea is an environmental justice issue, as the lake's recession poses significant air quality hazards for the disadvantaged local population. Mass fish die-offs and the exposure of lakebed playa to the beating sun promote sulfide emissions that contribute to high rates of asthma in nearby communities (Freund et al., 2022). Roughly 130,000 people live within 15 miles of the Salton Sea, a full third of which are children according to 2010 census data, making addressing this health hazard all the more crucial (Johnston et al., 2019). Local residents and ecosystems alike need drastic action taken to mitigate the worst effects of eutrophication and diminishing air quality in the area. Current dust suppression efforts focused on covering exposed playa with hay and tarps, and the recent expansion of the Salton Sea Species Conservation Habitat by the state government represent significant progress on this front, but the public health threat of the Sea's shrinkage persists (CDWR Staff, 2025). These health risks are an early example of the types of environmental hazards that shall become more frequent and severe around receding saline lakes as climate change accelerates, such as the Great Salt Lake in Utah or Lake Abert in Oregon (Johns Hopkins Staff, 2024). In this way, the Salton Sea serves as a case study for public health and environmental justice concerns over worsening air quality and extreme heat around drying saline lake ecosystems as climate change worsens.

Motivation:

This research project is ultimately grounded in concerns about dying ecosystems in increasingly aridifying areas and the subsequent health impacts on disadvantaged communities. Investigating climate and policy-driven compound heat and dust exposure around drying saline lakes like the Salton Sea is important for public health equity because those who often bear the highest cost of these hazards are ultimately the ones least responsible for them (Marlier et al., 2026). On a global level, industrialized nations have been responsible for roughly half of total historic greenhouse gas (GHG) emissions despite comprising only 12% of the global population, making them disproportionately the primary drivers of climate change (Popovich and Plumer, 2021). At the same time, these wealthy countries are the best equipped to weather the effects of climate change, while it is the less developed regions such as the Sahara and Central Asia that will contend with the greatest effects of climate-induced extreme heat and dry events (Zhang et al., 2022). The 2003 QSA-driven recession of the Salton Sea presents a similar case of environmental inequity. Water from the Imperial Valley agricultural sector was diverted to San Diego in order to support growing communities in the area, a region that is far wealthier and more prosperous than that of the Salton Sea. Policy choices made to specifically benefit more affluent communities came at a significant public health cost to some of the state's most disadvantaged and vulnerable residents. As such, an analysis of any disproportionate public health effects from climate and policy-induced compound exposure of extreme heat and dust in the area is warranted to assess the negative externalities of this water management regime.

Objectives:

This study examines three main knowledge gaps for compound heat and dust exposure in the Salton Sea region: determining what areas in the Salton Sea region are most affected by compound exposure, investigating how compound exposure in the area has evolved over time, and finally an examination of any disproportionate rates of compound exposure among more vulnerable local populations. Current literature on exact spatial distributions of compound exposure frequency around the Salton Sea is limited, and providing spatial maps of heat and dust co-exposure would be useful in illuminating regional health inequities and informing policy debates for hazard mitigation solutions. Determining how compound exposure has evolved temporally would also provide a timeline for how this environmental hazard has changed after the enactment of the 2003 QSA and the subsequent accelerated recession of the Salton Sea. Conducting disproportionality analyses on heat and dust co-exposure and associated respiratory disease is necessary as an issue of environmental justice and ensuring health equity, as current literature on exact rates of disproportionate exposure is lacking for the already underserved local communities.

Process Overview:

To achieve these research goals, this study examines various metrics for spatiotemporal extreme heat and dust compound exposure in the Salton Sea region using publicly available temperature, air quality, and health datasets. Data was processed in RStudio using the provided R script in this Google Drive folder. Results are in the form of static and interactive HTML maps, data CSVs, timeseries, and disproportionality plots of predefined compound exposure variables. Particular emphasis is placed on stratifying results by Social Vulnerability Index (SVI) quartiles to investigate any disproportionate impacts of compound exposure on disadvantaged populations. SVI is a 0-1 metric assigned to areas that account for adverse demographic and socioeconomic variables (e.g., poverty, transit access, housing availability, racial composition) to assess community preparedness for encountering hazards such as natural disasters and pandemics (CDC Staff, 2021). The rates of asthma in census tracts within the proximity of the Salton Sea with lower than state median annual household incomes were also processed in ArcGIS. In this way, any inequitable effects from heat and dust co-exposure may be revealed to better inform public policy and mitigation strategies in the Salton Sea region moving forward.

Data & Methods:
Data:

Aggregated California state overall SVI and SVI subthemes data for the years 2010, 2014, 2016, and 2018 was sourced from the CDC (CDC Staff, 2024). Biweekly average dust PM 2.5 concentration data in micrograms per cubic meter (µg/m^3) was sourced from van Donkelaar et al. for the years of 2000 to 2022 (Van Donkelaar et al, 2024). A proprietary shapefile of 157 predefined census tracts of the Salton Sea region was provided by Dr. Wenxin Lu of the University of California, San Diego's School of Public Health. Daily population-weighted mean temperature data in degrees Celsius was sourced from the PRISM Group (PRISM Staff, 2026). TIGER/Line shapefiles for California state census tracts were separately downloaded from the United States Census Bureau (Census Bureau, 2010). California statewide shapefiles for the percentage of adults with asthma and median annual household income were downloaded from SimplyAnalytics for the asthma public health portion of this analysis (SimplyAnalytics Staff, 2026).

Data was initially aggregated for spatial and temporal processing in RStudio. All necessary R libraries were installed and loaded into RStudio, and a polygon layer of the Salton Sea was downloaded from the US Census TIGER database for overlaying onto exposure maps. All aforementioned datasets were loaded into RStudio and cut down to the relevant study period of 2005 to 2022 (using the first 364 days of each year, including leap years, to obtain an even 26 biweekly periods per year for comparison). These datasets and shapefiles were then further filtered to the relevant 157 census tracts comprising the study area. Mean and max per-tract biweekly population-weighted average temperature, as well as 85th, 90th, 95th, and 99th percentile data for region and study period-wide temperature, were then processed. Per-tract extreme heat day counts across the study period were then calculated at each of these percentile thresholds. Region and study period-wide 75th and 90th percentiles for dust concentrations, as well as corresponding per-tract extreme dust day counts across the study period for each percentile threshold were then processed. These specific metrics and percentile thresholds were chosen to adhere to the compound exposure joint exceedance thresholds defined below. All of the above metrics were aggregated into a single combined dataframe.

Compound Exposure Metrics:

Compound Exposure Definitions:	Lower Joint Exceedance	Higher Joint Exceedance
Temperature:	At least 1 day above 89.6°F (regional 85th percentile) in a given biweekly period	At least 4 days above 89.6°F (regional 85th percentile) in a given biweekly period
Dust Concentration:	Above regional 75th percentile during same biweekly period as above	Above regional 90th percentile during same biweekly period as above

Figure 2. Table of temperature and dust concentration threshold definitions for lower and higher joint exceedance compound exposure metrics.

We used several different indices to determine when co-occurance of extreme heat and dust had been met. First, we calculated lower and higher joint exceedance as threshold-based binary indices. Lower joint exceedance for compound exposure was defined as when there is at least one day in a biweekly period in which temperature exceeds the regional 85th percentile of mean temperature and the overall dust concentration for that biweekly period exceeds the regional 75th percentile of dust concentrations. Higher joint exceedance for compound exposure was defined as when there are at least four days in a biweekly period in which temperature exceeds the regional 85th percentile and the overall dust concentration for that biweekly period exceeds the regional 90th percentile of dust concentrations. The frequency of compound exposure for lower joint exceedance was then calculated for each census tract by tallying every biweekly period where lower joint exceedance was met over the study period. Continuous indices were computed next, beginning with multiplicative interaction, where each tract-biweekly period dust datapoint was multiplied by the number of extreme heat days in that biweekly period. Additive z-score indices were then calculated, where tract-biweekly dust and heat data points were all standardized to their corresponding z-scores and then summed. Percentile-percentile products were processed next, with dust and heat tract-biweekly periods being converted to their respective percentile ranks relative to the entire region and study period, and then multiplied together. Cumulative and persistence measures were then calculated, where runs of 2+ consecutive biweekly periods of the threshold for lower joint exceedance being met were flagged and then summed across the study period for each census tract. Cumulative compound burden per year for each census tract across the study period was next calculated for each of the aforementioned continuous indices by summing all data points for each calendar year per index. Summer seasonal compound burden was processed using this same approach, but restricted to biweekly periods falling during the summer period of June 21st to September 22nd of each calendar year.

Visualization and Analysis:

Claude A.I. was utilized to first optimize the written aggregation and compound exposure statistics calculations code for faster processing. Claude was then used to generate code for every data visualization in the "Results" section of this paper. Detailed prompts and back-and-forth questioning were utilized to ensure exact, correctly coded visualizations for proper analysis. The full Claude chat history is accessible via this link, and all used and unused data visualizations, CSVs, ArcGIS data, and interactive HTML maps are accessible via this previously linked Google Drive folder.

The 2014 SVI data was used for SVI overlays since it falls directly in the middle of the 2005-2022 study period. Tracts were all grouped by SVI quartile, meaning an uneven number of tracts were grouped into the 0-0.25, 0.25-0.5, 0.5-0.75, and 0.75-0.1 SVI ranges. Out of all 157 tracts in the study region, 24 fell in the first quartile, 41 in the second, 42 in the third, and 50 in the fourth. Each time series, disproportionality analysis, and compound exposure graph were stratified by SVI quartile to assess any disproportionate rates of hazard exposure among vulnerable communities. SVI data is included in the bivariate choropleth map as well.

For visualizations for the asthma portion of this analysis, shapefiles were loaded into ArcGIS and then reprojected to the 0406 projection using the "Project" tool. A polygon outline of the Salton Sea was created in the Editor toolbar using the "Imagery" basemap as a reference. For Figure 20, census tracts that were above the state average for the percentage of adults with asthma were extracted by utilizing the "Select by Attribute" geoprocessing tool and creating a new layer. Tracts were differentiated into seven categories using a graduated color histogram symbology template, which was also used to find the average value for this dataset. The same process was used for Figure 21, but for census tracts that were below the state median annual household income level. This involved exploring the household income dataset's attribute table by clicking "Explore Statistics" to find the median value. The "Pairwise Clip" tool was used to create a layer of census tracts that were both above the state average for asthma and below the state median annual household income level. These tracts were again differentiated into seven categories by annual household income level using a graduated color histogram symbology template.

Results:
Heat Visualizations:

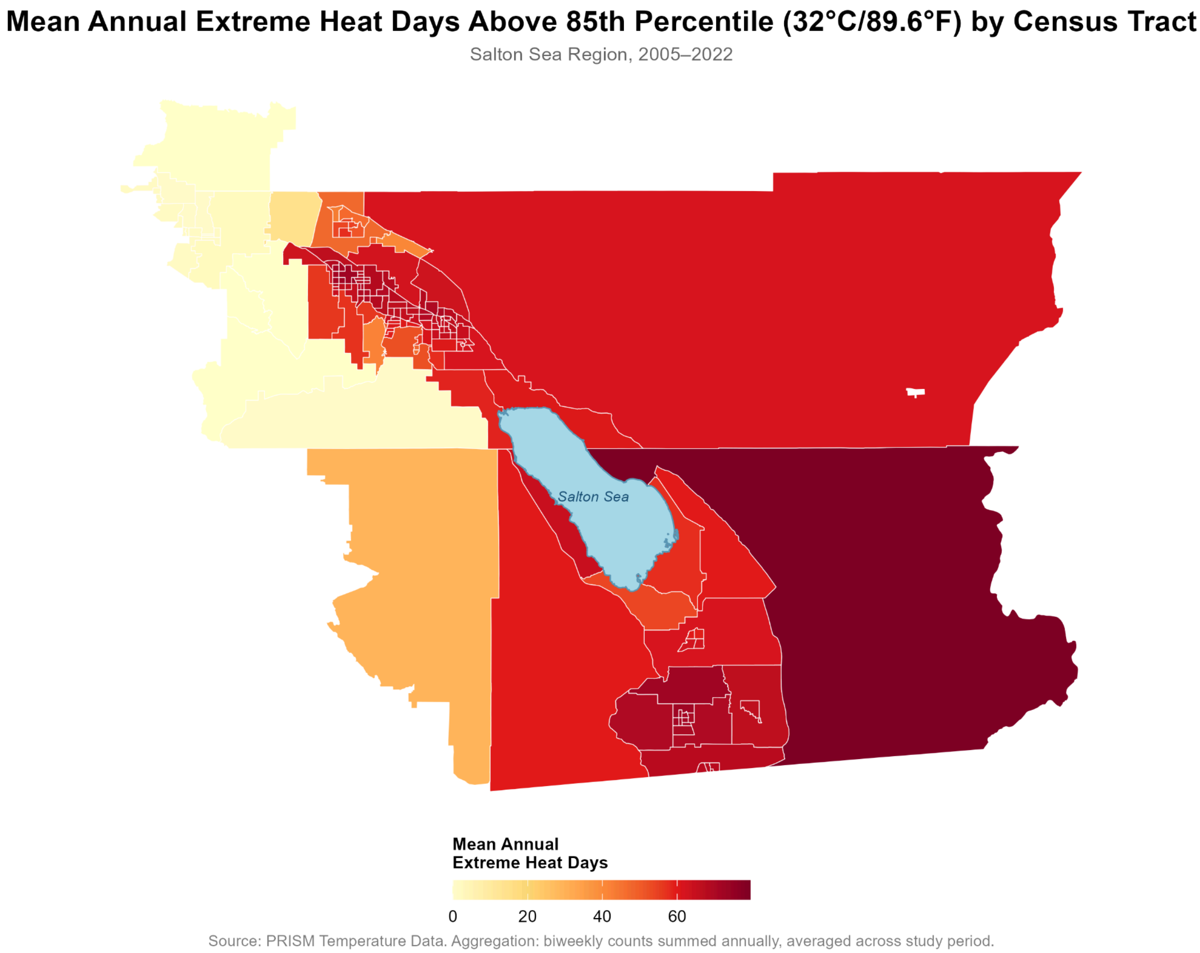

Figure 3. Mean annual days above 85th percentile regional temperature across study period by census tract.

We found that 134 out of 157 (or 85.4%) of the analyzed census tracts in the Salton Sea region experienced more than 25 days above the regional 85th percentile for daily population-weighted mean temperature (32°C/89.6°F) in an average year over the study period (Figure 3). We see an even higher number of extreme heat days in the southern census tracts near the border and in the upper Coachella Valley. The reddest census tract in the southeast in particular approaches nearly 80 days out of a given year above the 32°C threshold for extreme heat. Notably, the tracts in the northwest near Beaumont, Riverside, and Redlands all had less than 3 extreme heat days in an average year.

Dust Visualizations:

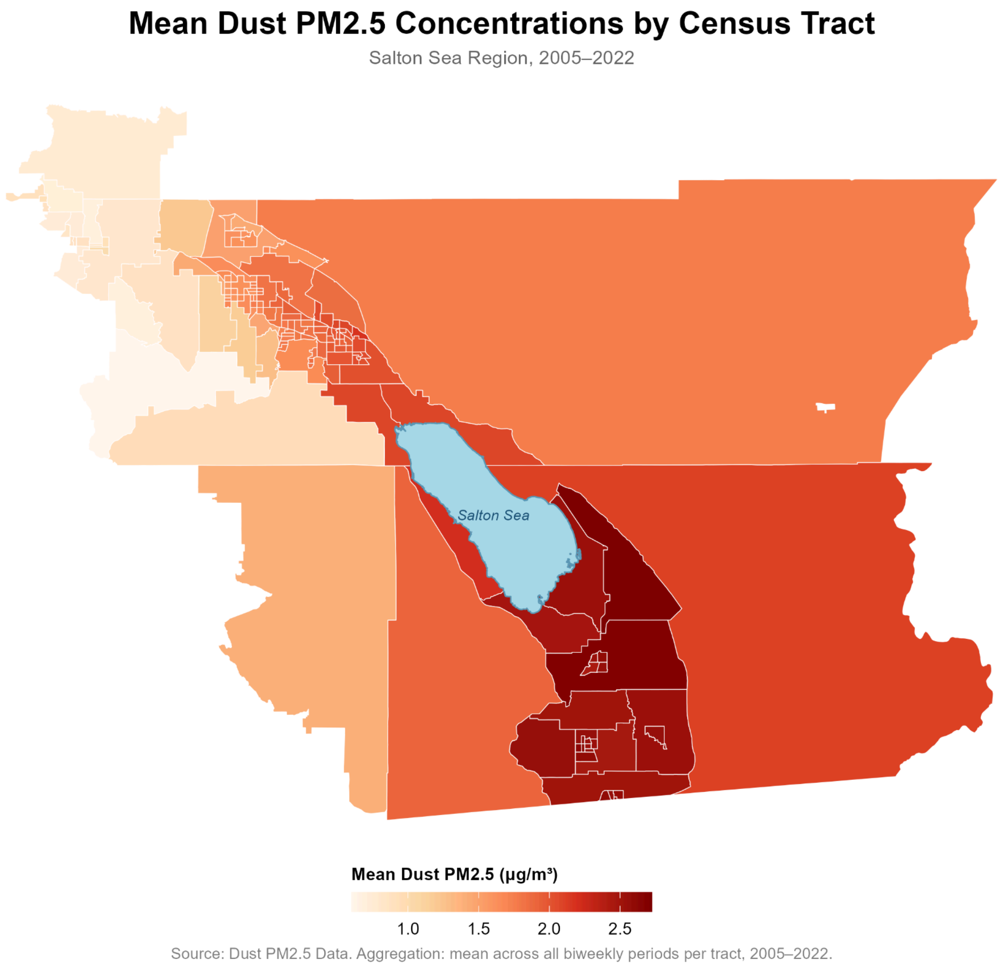

Figure 4. Mean dust PM 2.5 concentration (µg/m^3) across the study period by census tract.

We found that air quality is much worse in the southern part of the study region, with the most darkly shaded tracts ranging from roughly 2.5-2.7 µg/m^3 of mean dust PM 2.5 concentration, while tracts outside of this area typically fell in the 1.4-2.2 µg/m^3 range (Figure 4). The exception to this was once again the northwestern portion of the study region where overall exposure was far less severe, with concentrations falling within the roughly 0.7-1.2 µg/m^3 range. This spatial pattern in dust exposure was observed likely in part because the southern part of the study region is often downwind of the Sea. The Salton Sea itself is bordered by the Santa Rosa Mountains to the west and the Chocolate Mountains to the east, and this acts as a wind tunnel for winds to blow northwest to southeast, potentially scattering regional dust southward (Evan, 2019).

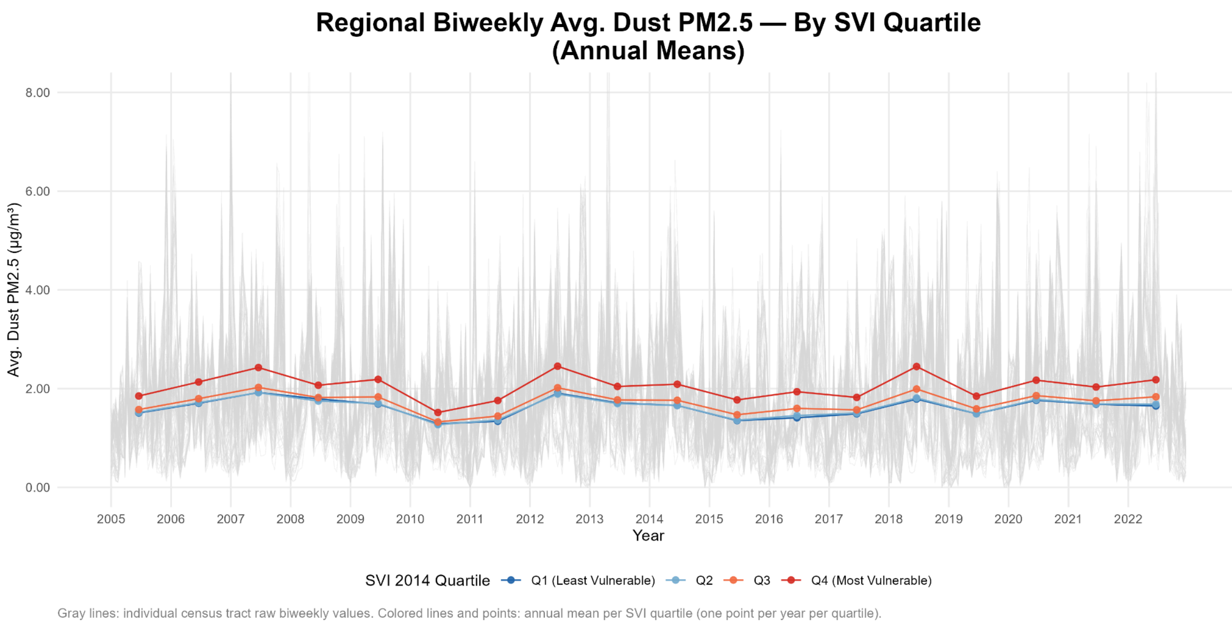

Figure 5. Biweekly average dust PM 2.5 concentration (µg/m^3) across the study region, with annual means stratified by SVI quartile.

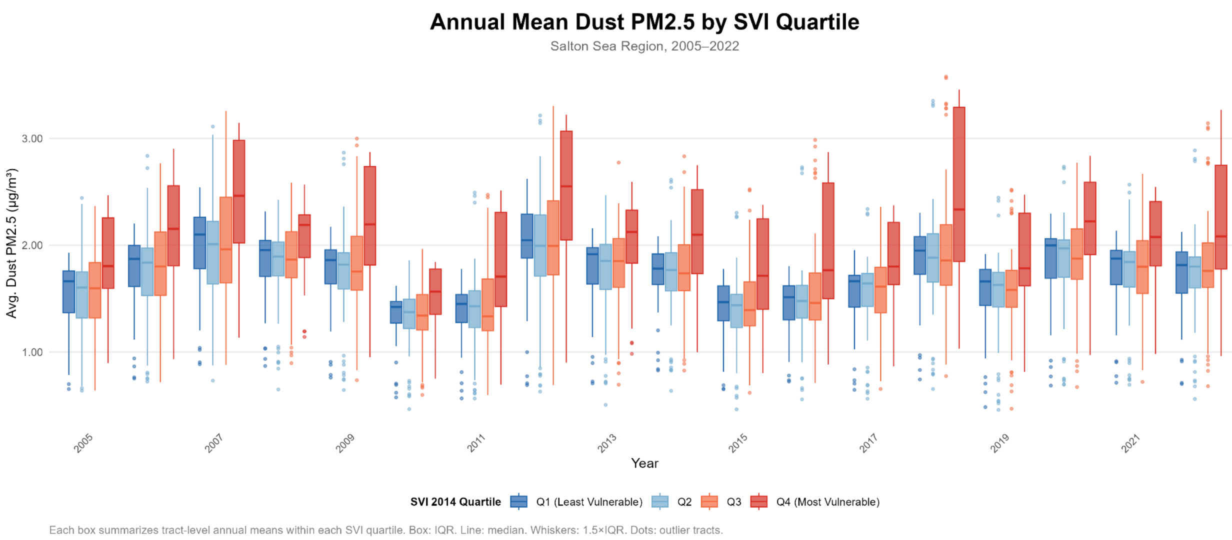

Figure 6. Boxplots of annual mean dust PM2.5 (µg/m^3) across the study region and period, stratified by SVI quartile.

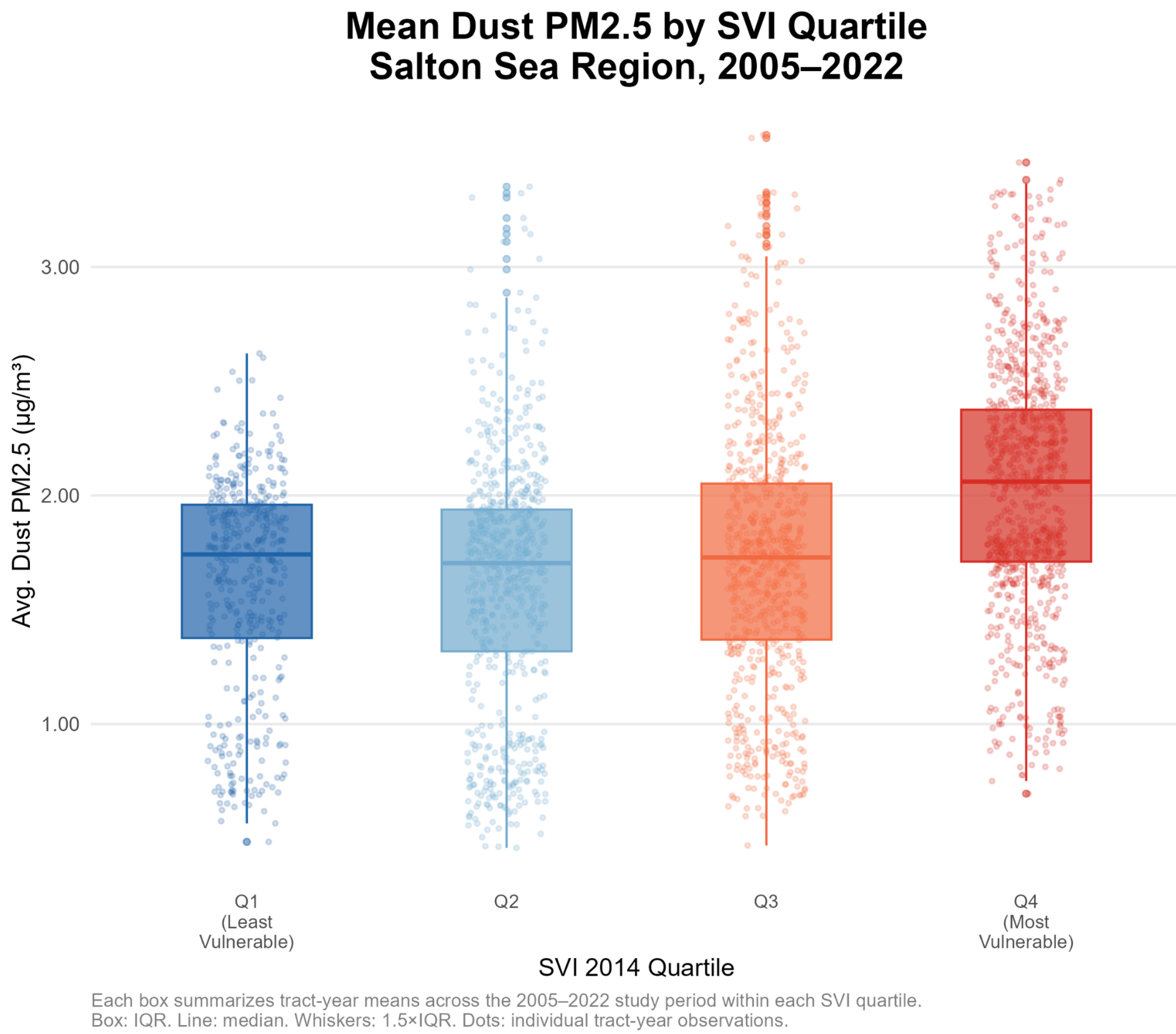

Figure 7. Boxplots of mean dust PM2.5 (µg/m^3) across the study region and period, stratified by SVI quartile.

We found that the most vulnerable areas around the Salton Sea also have to contend with the worst air quality, with individuals falling within the red upper fourth quartile of the 2014 SVI bearing a far higher level of dust exposure than the other 3 less vulnerable quartiles of the population (Figures 5-7). This most vulnerable quartile contended with roughly 2.1 µg/m^3 of dust concentration on average over the study period, while this number falls to only approximately 1.7 µg/m^3 for the other 3 population quartiles. The upper bounds of the fourth quartile SVI data points in the annual means graph, in particular, far exceeded those of the rest of the SVI groups.

Compound Exposure Visualizations:

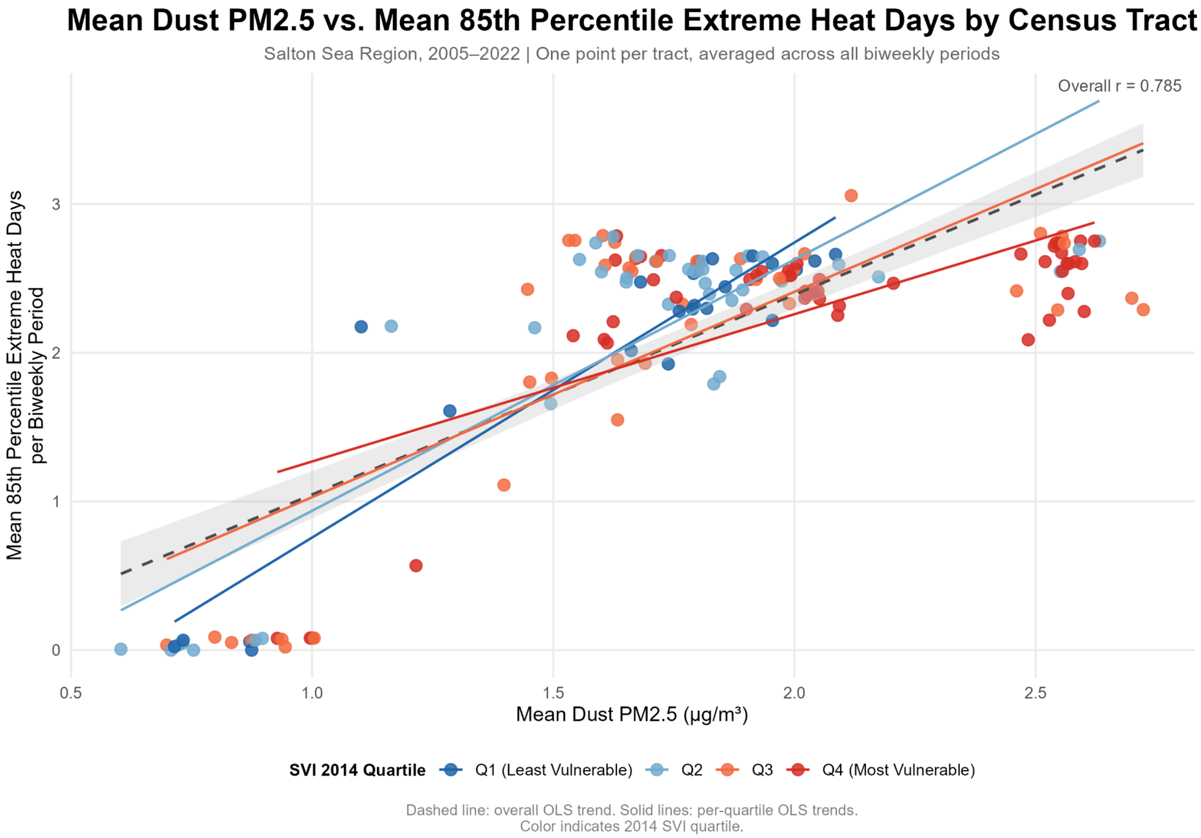

Figure 8. Ordinary Least Squares Fit (OLS) of mean per-tract dust PM 2.5 (μg/m^3) concentration versus mean number of days in a biweekly period in each census tract exceeding the 85th percentile of population-weighted mean temperature across the study region, stratified by SVI quartile.

We found that the mean per-tract dust PM 2.5 concentration and mean biweekly extreme heat days displayed notable positive correlation across the study region (Figure 8). With a high r-value of 0.785, these two variables are highly positively correlated with one another, meaning the presence of one is associated with the presence of the other. This shows that areas with a higher average level of extreme heat days also generally contend with higher levels of dust concentration, indicating a higher probability of compound exposure.

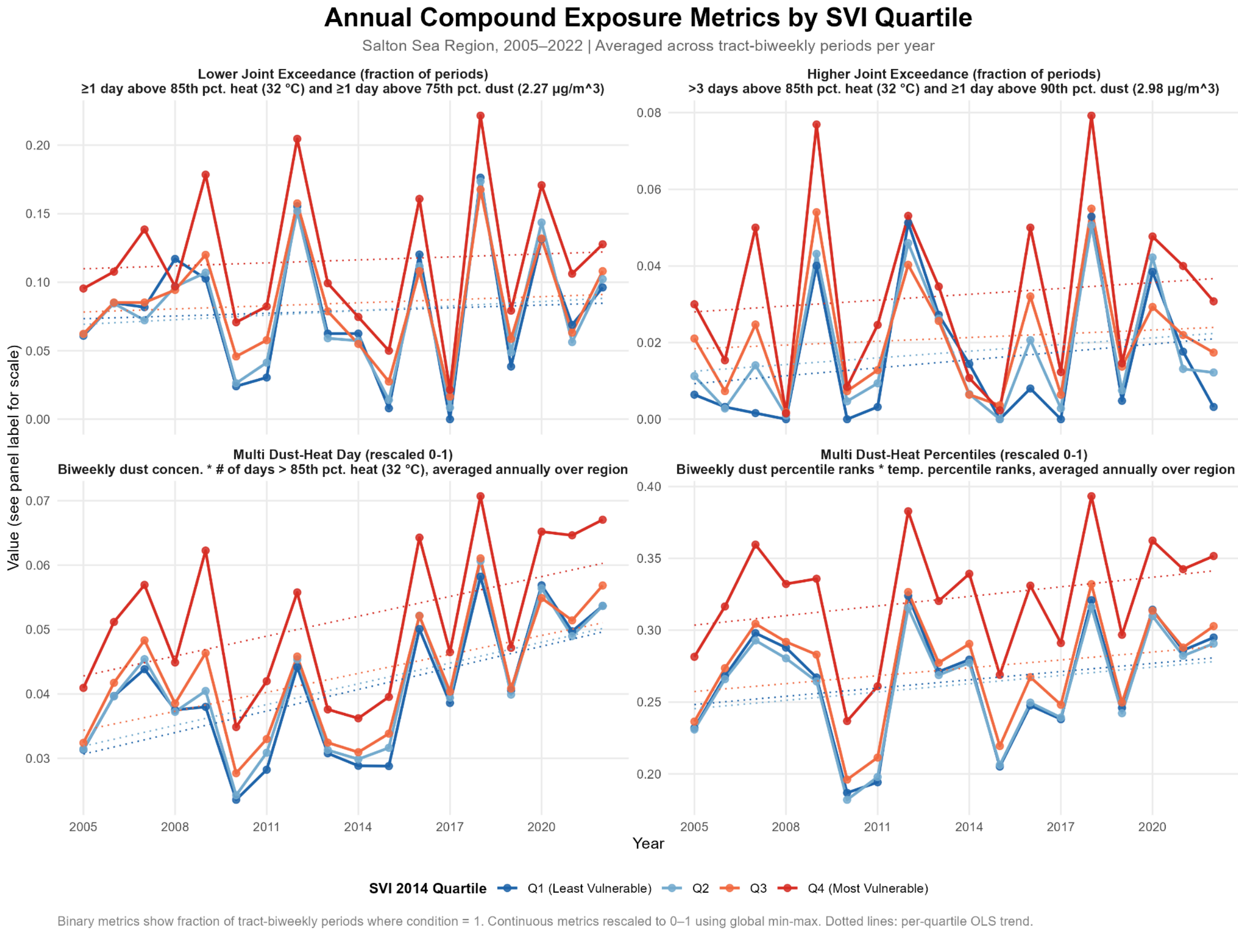

Figure 9. Average annual fraction of tract-biweekly periods experiencing compound exposure metrics, stratified by SVI quartile.

We found that populations falling in the upper fourth quartile of SVI exhibit an elevated level of compound exposure across every calculated metric compared to the other SVI quartiles (Figure 9). These graphs also indicate a generally upward trend in compound exposure over time in the region across every metric, particularly for the multi-dust heat day and multi-dust-heat percentiles indices.

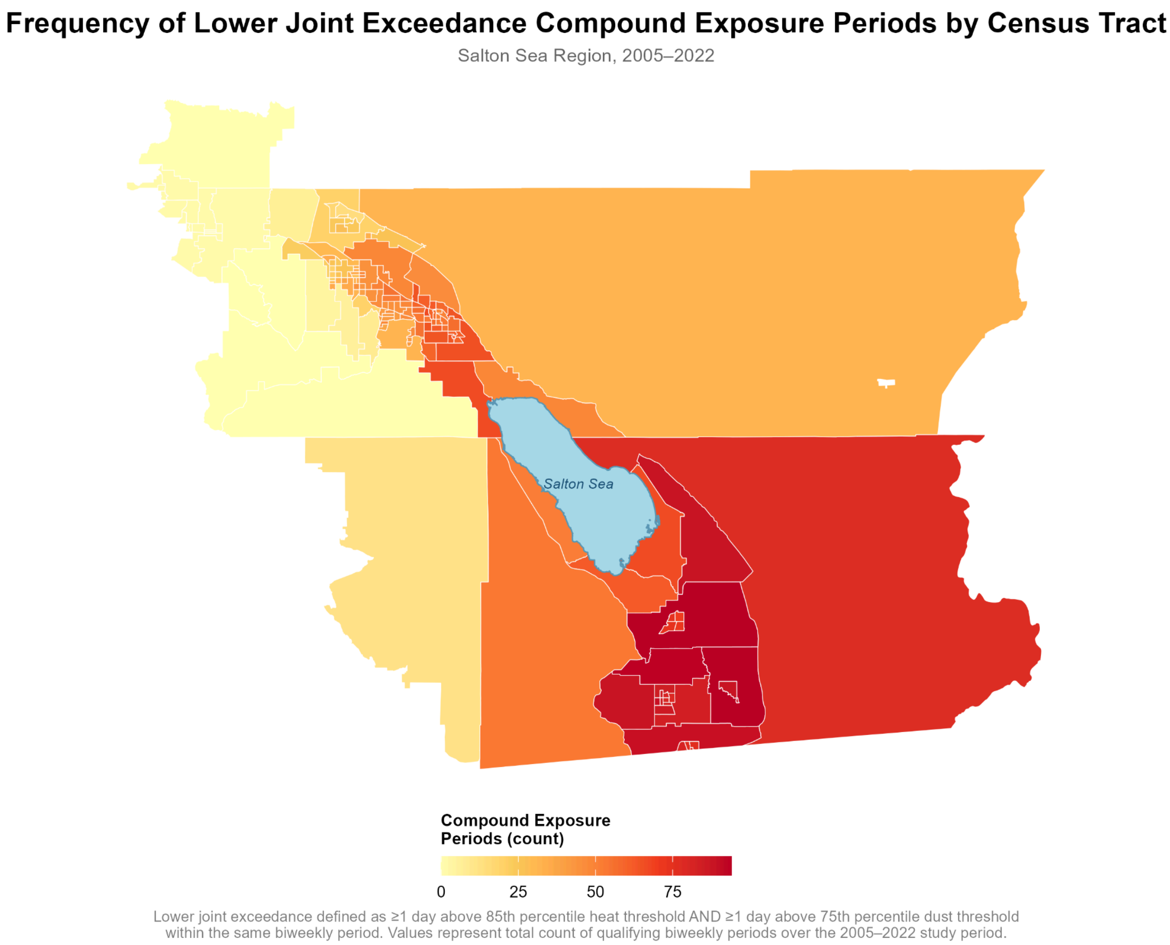

Figure 10. Number of biweekly periods exhibiting lower joint exceedance for compound heat-dust exposure by census tract.

We found that the southern part of the study region once again most often has to contend with poor air quality and extreme temperatures concurrently. Tracts directly south of the Salton Sea had roughly 90 biweekly periods (or nearly 20% of all those examined in the study period) meet the lower joint exceedance threshold for compound exposure (Figure 10). This is again contrasted by the northwest portion of the region, where compound exposure periods numbered at either 0 or in the low single digits across the study period. Regional dust exposure seems to be primarily associated with the above compound exposure trends, as this graphic exhibited a very similar spatial pattern to the dust exposure map (Figure 3) and less so to the heat exposure map (Figure 2).

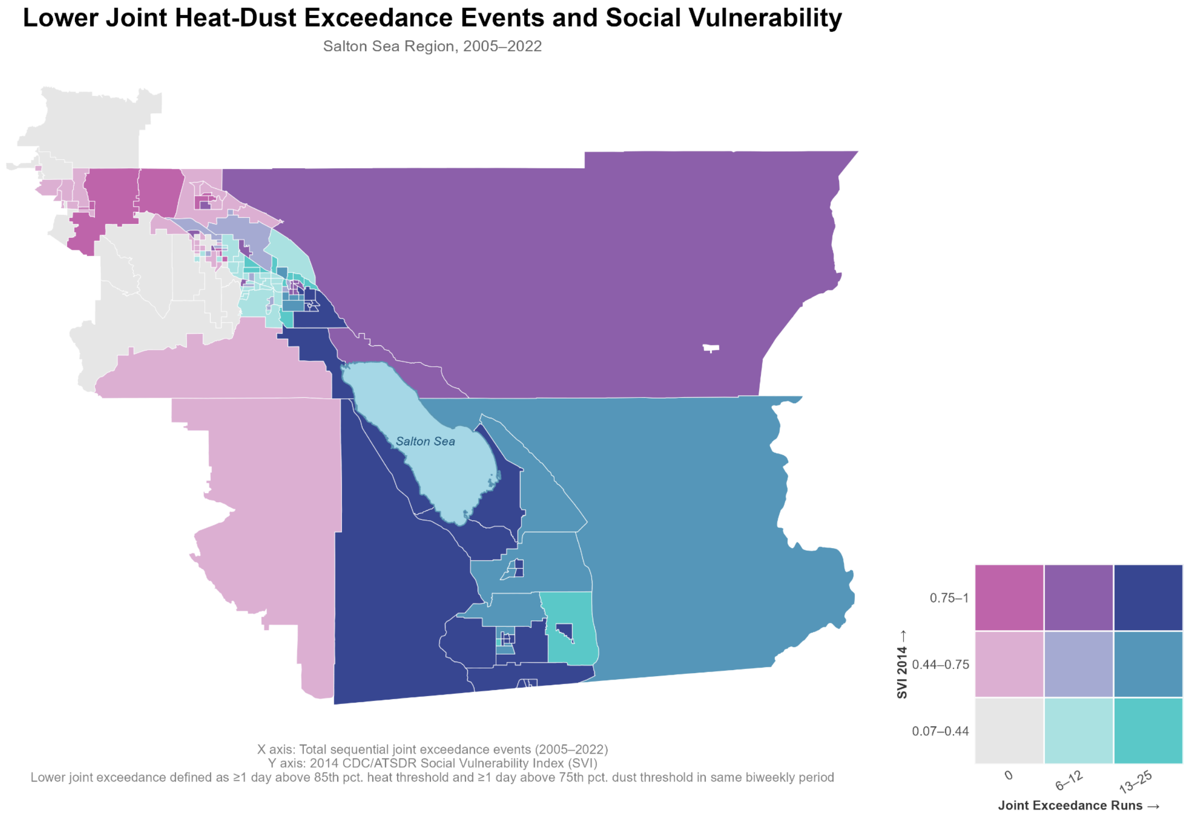

Figure 11. Bivariate choropleth of total sequential periods of joint heat-dust exceedance events over the study period versus SVI, by census tract.

We found that many of the tracts bordering the Salton Sea and to the south of the study region in dark blue exhibited high social vulnerability and high levels of cumulative compound exposure concurrently (Figure 11). The "joint exceedance runs" metric mapped above is essentially a count of how many total instances there are of 2 or more back-to-back biweekly periods that exceed the lower joint exceedance threshold over the study period. This indicates areas that contend with sustained periods of co-exposure rather than isolated spikes in compound exposure. The most consistently co-exposed and socially vulnerable sections in dark blue all contended with over a dozen instances of back-to-back compound exposure periods over the study period. Since extreme heat days mostly occur during the summer season, this points to these areas contending with sustained periods of co-exposure likely during this portion of the year. Notably, tracts to the northwest, closer to Riverside and Redlands, had zero runs of compound exposure periods over the entire 18-year study period.

Disproportionality Analyses:

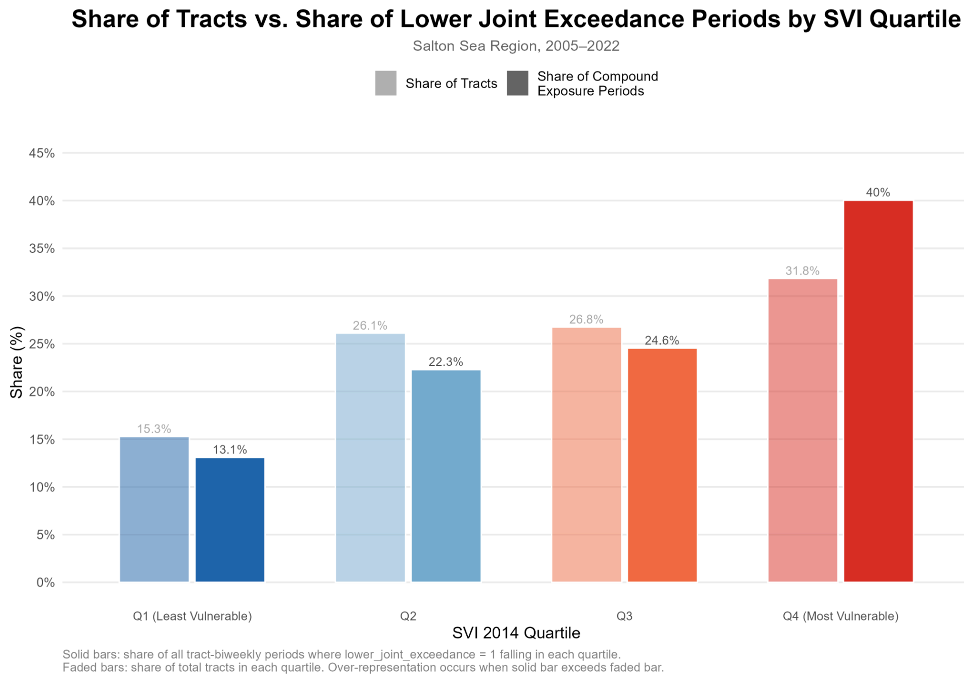

Figure 12. Disproportionality analysis grouped bar chart of share of tracts in each SVI quartile versus share of total lower joint exceedance compound exposure periods experienced by those tracts in each SVI quartile over the study period.

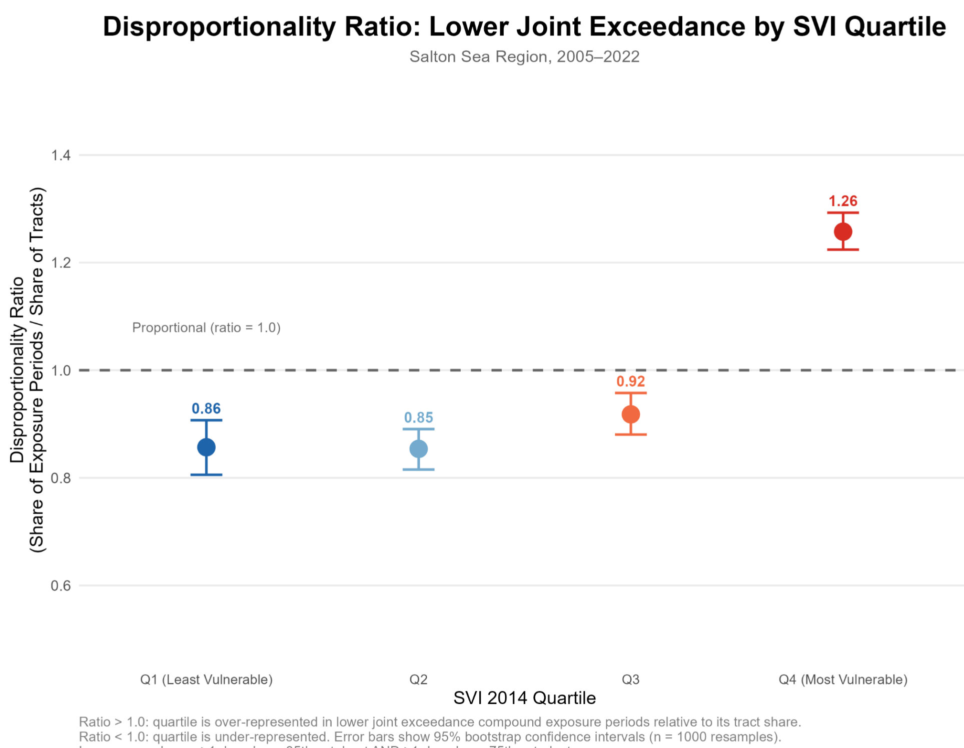

Figure 13. Disproportionality analysis ratio plot of share of tracts in each SVI quartile vs. share of total lower joint exceedance compound exposure periods experienced by those tracts in each quartile over study period.

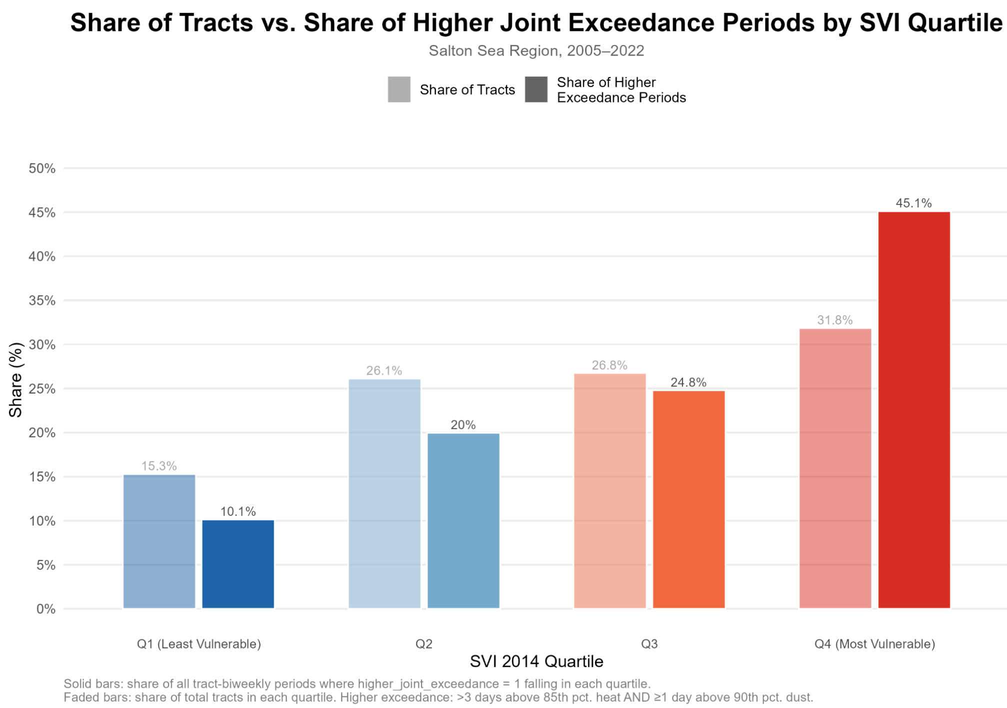

Figure 14. Disproportionality analysis grouped bar chart of share of tracts in each SVI quartile versus share of total higher joint exceedance compound exposure periods experienced by those tracts in each SVI quartile over the study period.

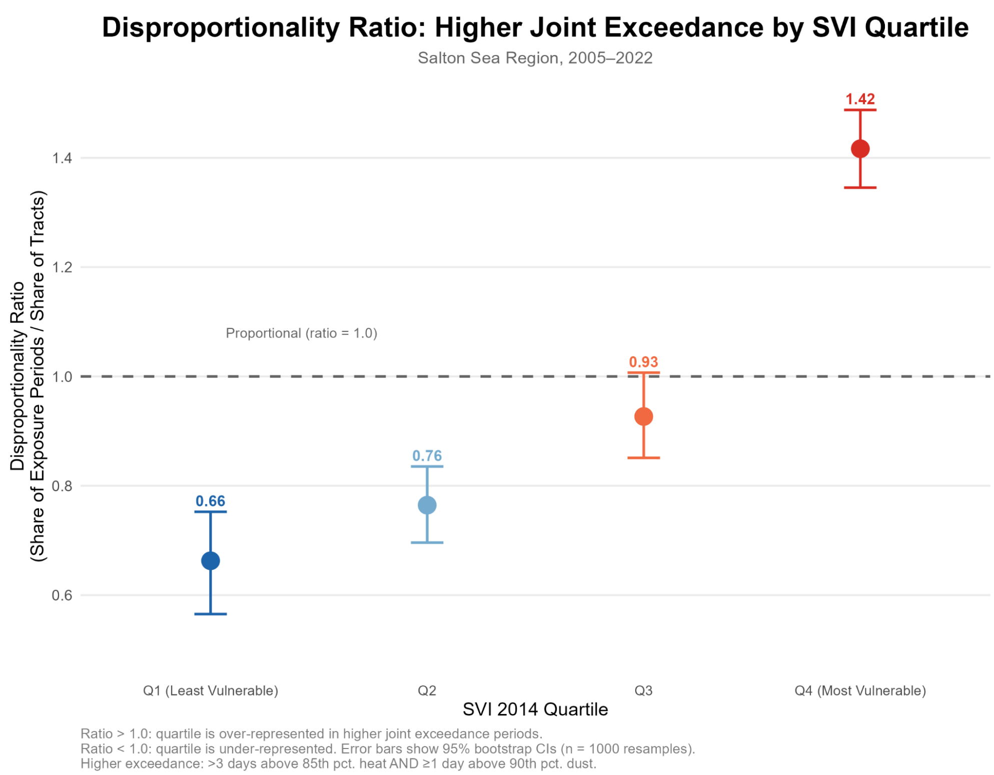

Figure 15. Disproportionality analysis ratio plot of share of tracts in each SVI quartile versus share of total higher joint exceedance compound exposure periods experienced by those tracts in each SVI quartile over the study period.

We found that the most vulnerable populations in the study region (in red) are the most exposed to poor air quality and extreme heat concurrently, with these populations bearing 26% higher compound exposure periods than they theoretically should given their overall portion of the population (Figures 12-15). This is especially true for higher degrees of compound exposure, as the relationship between higher SVI and disproportionate co-exposure becomes markedly stronger across the four population quartiles at the higher joint exceedance level. This is particularly true for populations in the upper 4th SVI quartile, where these tracts are now bearing 42% greater compound exposure periods than they should in a completely health-equitable scenario. Findings in disproportionate exposure like this are made even more notable because nearly a third (31.8%) of census tracts in the region fell into this highest SVI quartile.

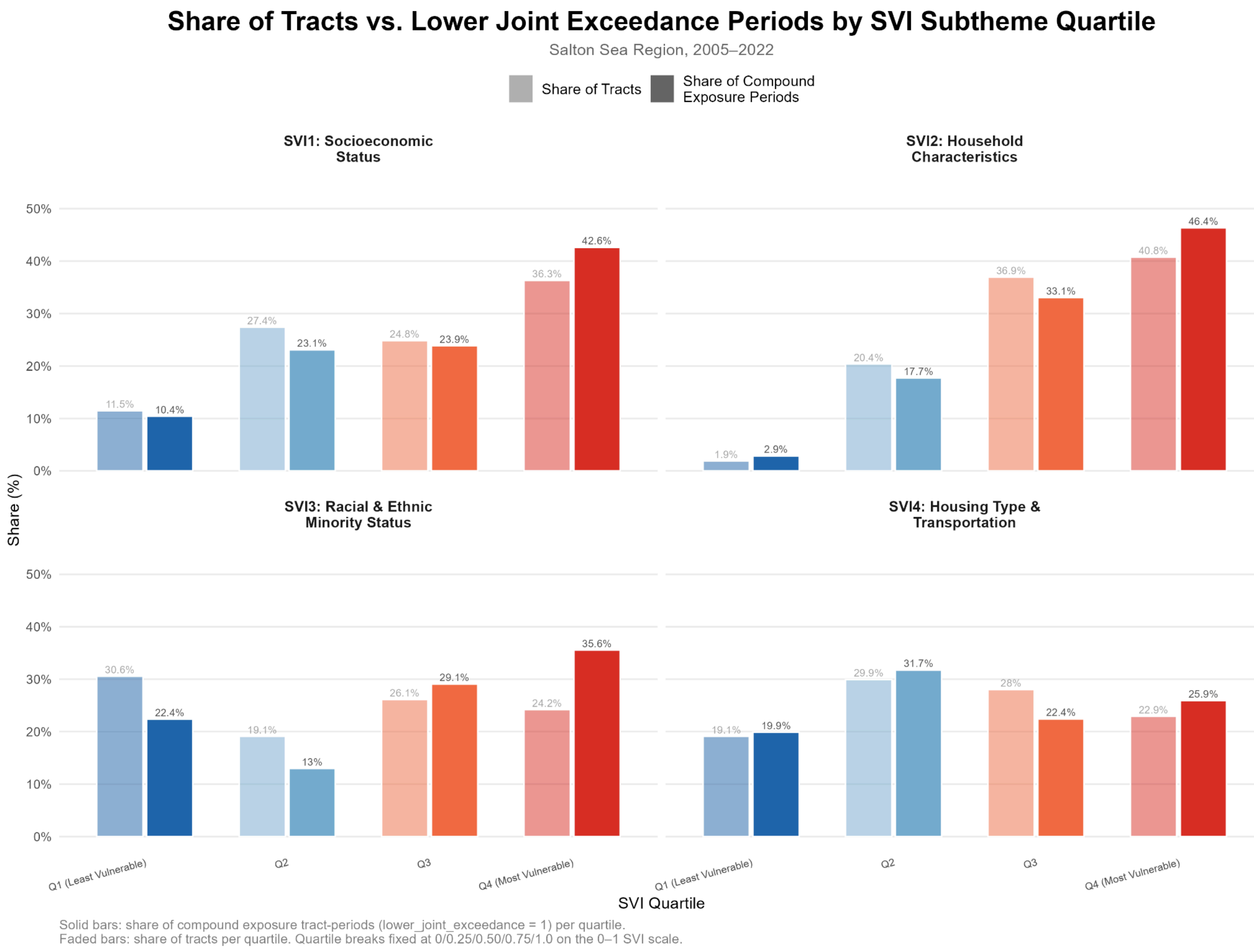

Figure 16. Disproportionality analysis grouped bar charts of share of tracts in each SVI quartile versus share of total lower joint exceedance compound exposure periods experienced by those tracts in each SVI quartile over the study period, for each SVI subtheme.

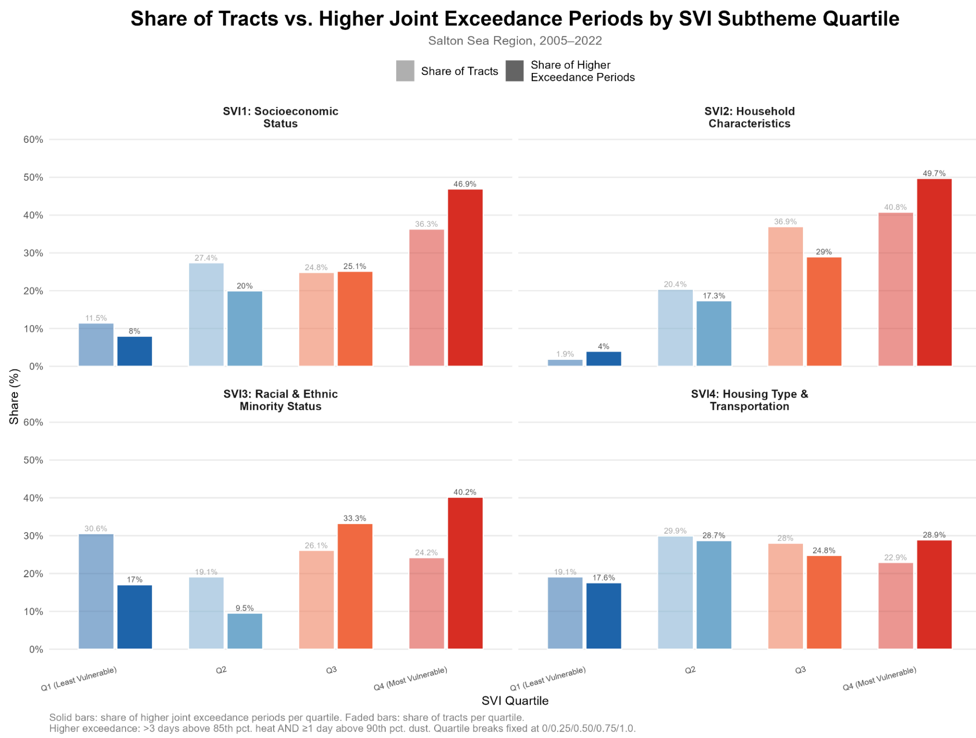

Figure 17. Disproportionality analysis grouped bar charts of share of tracts in each SVI quartile versus share of total higher joint exceedance compound exposure periods experienced by those tracts in each SVI quartile over the study period, for each SVI subtheme.

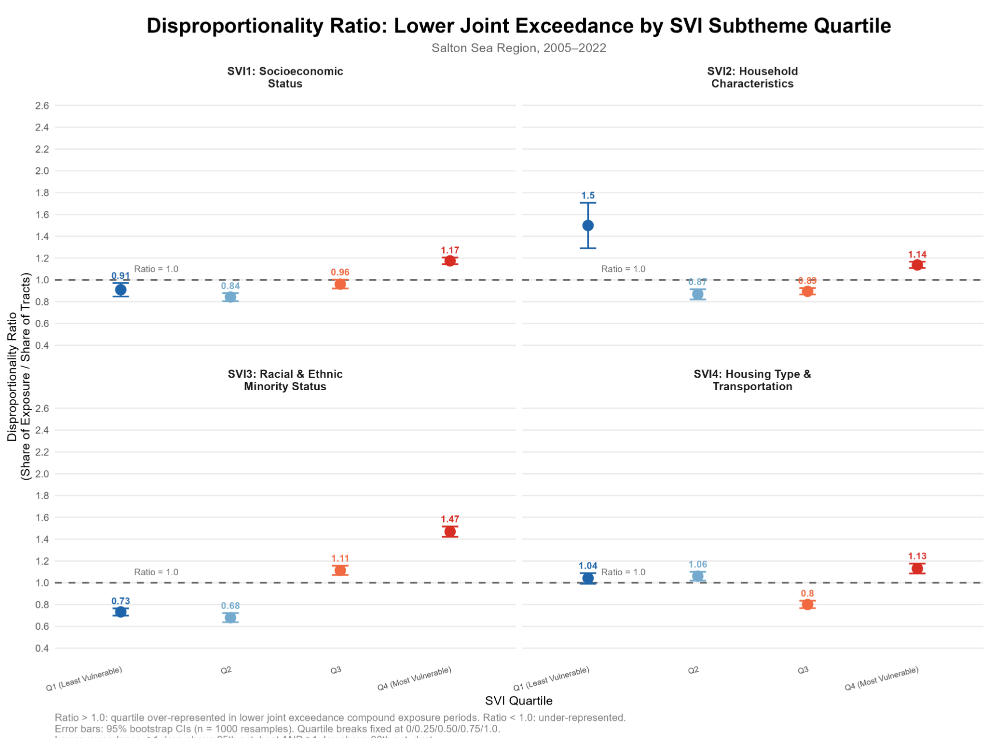

Figure 18. Disproportionality analysis ratio plot of share of tracts in each SVI quartile versus share of total lower joint exceedance compound exposure periods experienced by those tracts in each SVI quartile over the study period, for each SVI subtheme.

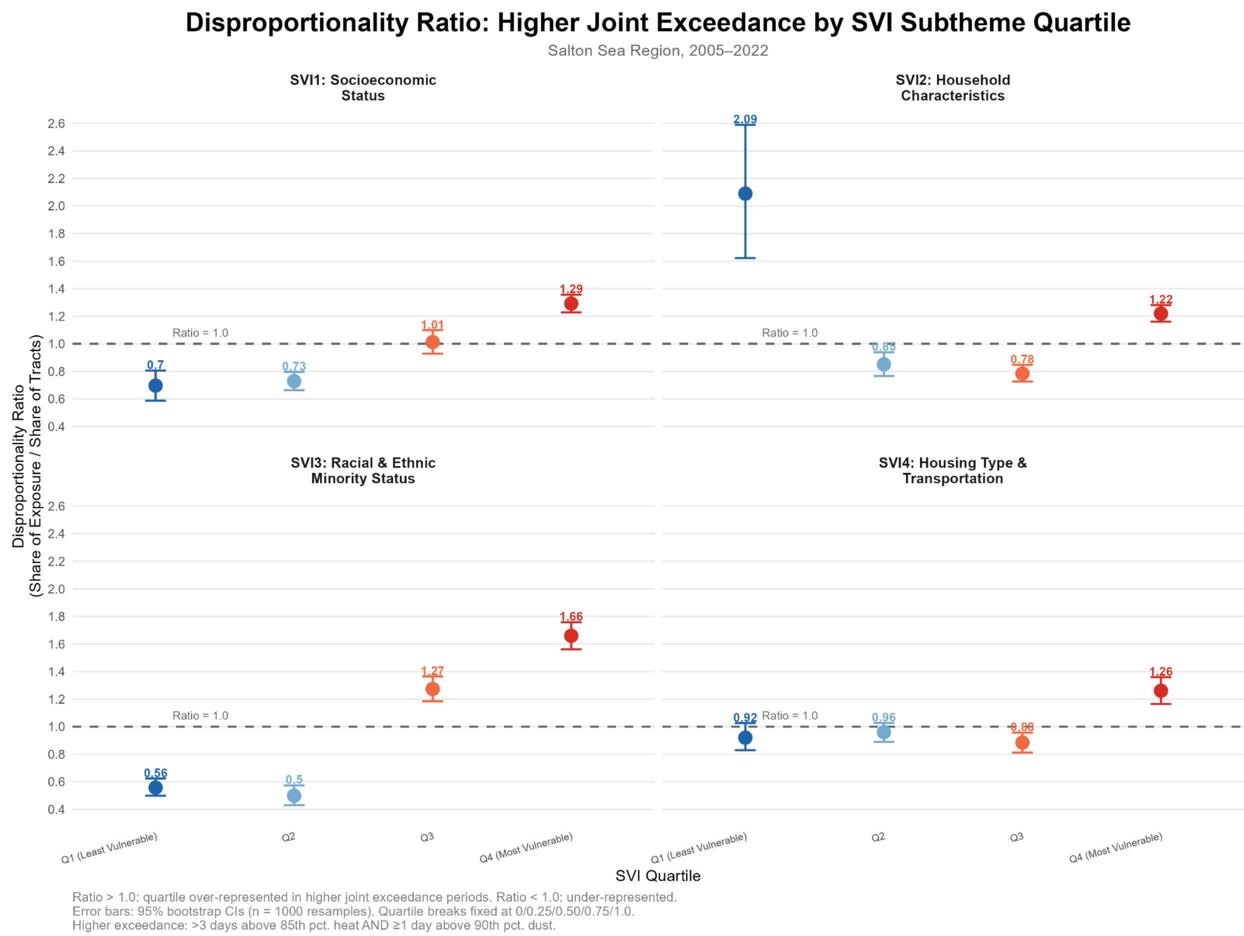

Figure 19. Disproportionality analysis ratio plot of share of tracts in each SVI quartile versus share of total higher joint exceedance compound exposure periods experienced by those tracts in each SVI quartile over the study period, for each SVI subtheme.

We found that when the overall 2014 SVI is broken down by subtheme, racial and ethnic minority status emerges as the primary demographic predictor of disproportionate co-exposure in the study region, with the most vulnerable 4th quartile of this demographic group bearing 47% higher compound exposure periods than they would in a completely health-equitable scenario (Figures 16-19). Socioeconomic status, household characteristics, and housing type and transportation subthemes all displayed more muted trends. Notably, the level of co-exposure by SVI quartile becomes even more disproportionate for each of the four subthemes at the higher joint exceedance level, with the most vulnerable racial and ethnic minorities bearing 66% greater higher joint exceedance compound exposure periods than they should compared to their portion of the overall population.

Asthma Analyses:

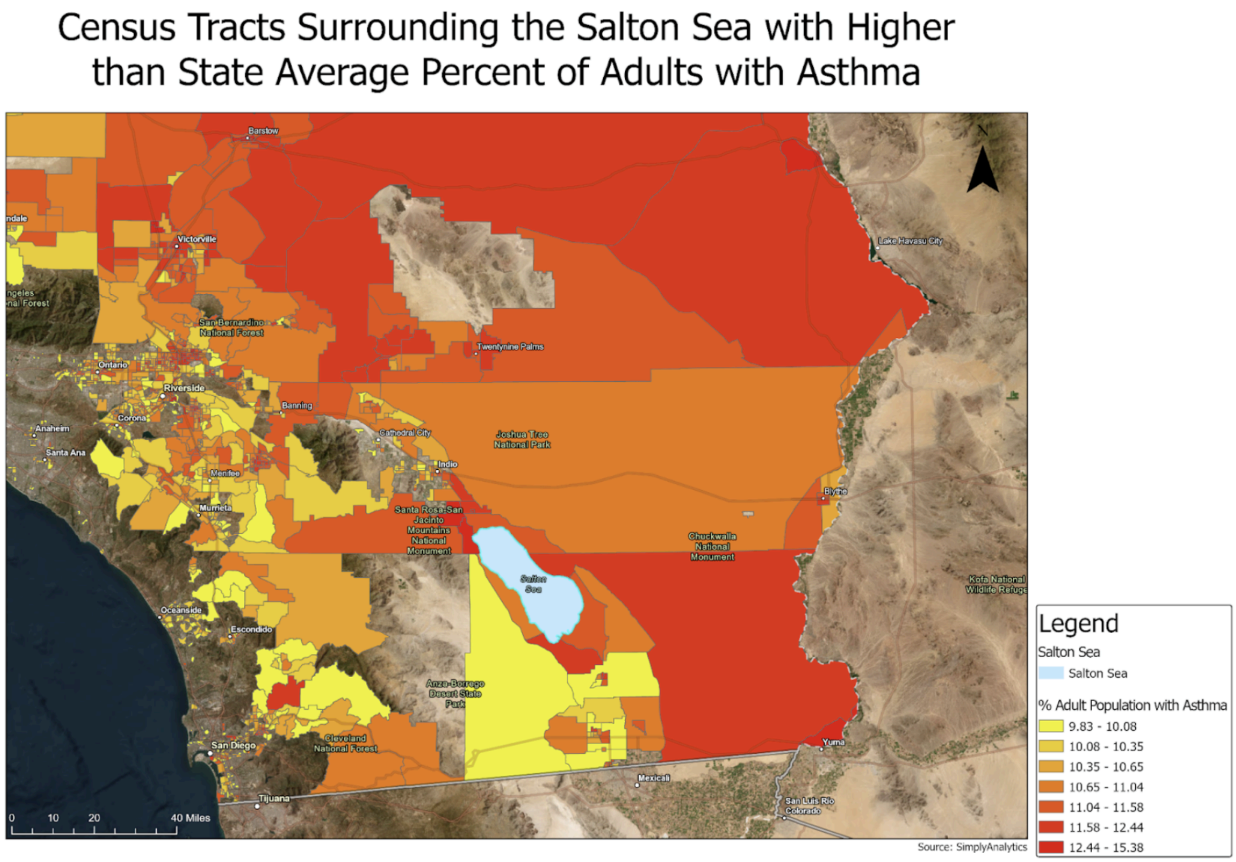

Figure 20. Surrounding census tracts exhibiting higher than California state average asthma rates in adults.

We found that census tracts immediately surrounding the Salton Sea and to the southeast exhibit some of the highest rates of asthma in the state, with rates as high as roughly 15% (Figure 20). This fits with the overall displayed trend of the more rural Eastern half of Southern California exhibiting much higher rates of asthma than the more populous Western and coastal region. This also aligns with the spatial patterns of dust concentration displayed in Figure 4, where higher tract-level dust concentrations are associated with an increase in the risk of asthma in locals, particularly in more populous places like Imperial City. Notably, many census tracts in the study region were represented here, meaning that they all exhibit asthma rates exceeding the state average of roughly 9.8%.

Below State Median Household Income Census Tracts Surrounding the Salton Sea with Higher than State Average Percent of Adults with Asthma

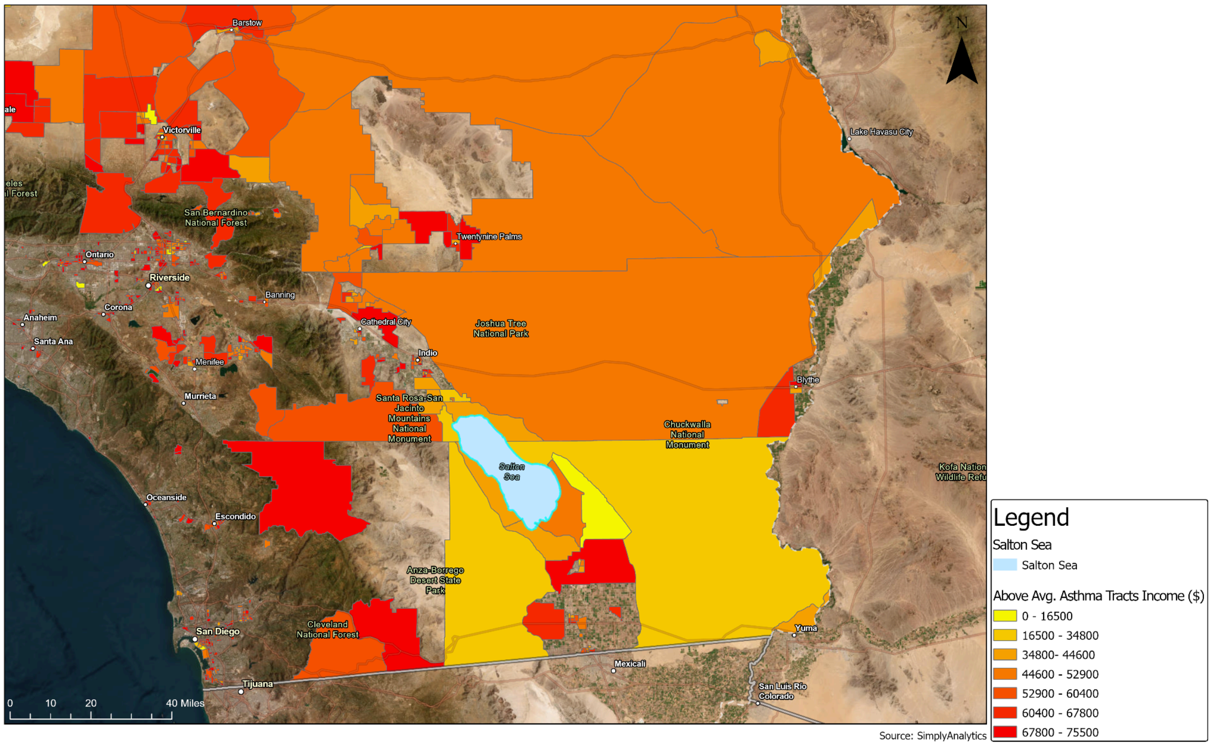

Figure 21. Surrounding census tracts exhibiting higher than the California state average asthma rates in adults that are below the state median annual household income level, sorted by annual household income.

We found that many of the same census tracts immediately surrounding the Salton Sea and in the Eastern half of the state that display high rates of asthma are also some of the poorest in the area by annual household income (Figure 21). This is particularly true for the tracts bordering the Sea and to the Southeast. There were demonstrably higher rates of respiratory disease among the poorest populations in the Salton Sea region, with many tracts exhibiting asthma rates approaching 15% in adults also falling within the three lowest income segments and thus below $45,000 in annual household income. These demonstrated health impacts of low air quality in the area align well with prior maps, disproportionality plots, and time series evaluating compound exposure levels by 2014 SVI.

Discussion:

Conclusions:

Our results suggest that compound exposure of extreme heat and dust is increasing over time in the Salton Sea region (Figure 9), reflecting broader trends of aridification and increasing temperatures across the western US. We also find that regions with higher average extreme heat days also experience elevated levels of dust. The more rural and arid eastern regions of the Salton Sea area and Southern California as a whole exhibited higher rates of co-exposure to extreme heat and dust, as well as correspondingly elevated levels of asthma relative to the more temperate western region closer to the coast. The southern section of the study area, in particular, is the most negatively impacted by compound exposure events. This is largely spatially associated with dust exposure, since the pattern of dust exposure in Figure 4 closely aligns with the compound exposure pattern observed in Figure 10. This suggests that these tracts are likely most affected by dust exposure due to being downwind of the region's wind tunnel, where overall regional dust emissions then accumulate. However, without particle tracing to track the movement of dust particles from the exposed Salton Sea playa to these areas during a dust storm event, specific causal effects from the lake's decline cannot be firmly established.

Each of the presented SVI stratified time series, disproportionality analysis, and asthma rate by income level maps reinforces that the most disadvantaged communities in the region bear the highest exposures and adverse health effects. This is especially true of the most extreme events, as disproportionality in rates of compound exposure periods grows notably larger when limiting this to higher joint exceedance co-exposure periods. Racial and ethnic minority status is by far the most strongly associated with inequitable dust and heat exposure trends out of all four analyzed subthemes of the 2014 SVI. This level of inequality in compound exposure, particularly among racial and ethnic minorities in the region, poses serious environmental justice concerns. The Salton Sea region already skews towards the higher SVI quartiles, potentially because wealthier, less disadvantaged individuals can choose to move away to escape the health hazards prominent in the area, leading to the overall regional population being substantially more socially vulnerable than the national average over time. As compound exposure events become more frequent, given accelerating climate change trends and the continued recession of the Salton Sea, this level of disproportionality in public health hazard exposure will likely become increasingly untenable for the region.

The provided asthma rate analysis maps reveal that census tracts closer to the Salton Sea exhibited some of the highest rates of asthma in the state. This again reinforces the hypothesis that the continued recession of the Salton Sea and increased playa exposure to dust storms are driving decreased air quality in these areas, which in turn results in increased rates of respiratory disease among residents. Additionally, many of the census tracts surrounding the Salton Sea that were above the state average rate for asthma were also below the state median household income level. This indicates that the low air quality from the sulfuric dust spread by the shrinking Salton

Sea is leading to disproportionately higher rates of asthma among low-income communities in the area. Elevated negative public health effects among poorer populations reinforce the Sea's decline as an issue of environmental justice, although again, causation cannot be firmly established without further research.

Limitations:

Several limitations to this research study must be acknowledged as potential caveats to the presented results and conclusions. The primary limitation is that pre-2005 and more recent years aren't represented in the aggregated dataset. Having pre-2003 QSA data in the study period (e.g., beginning in 2000) as well as data for the last several years would provide a more holistic view of both the ongoing public health concerns in the region as well as the decline of the Salton Sea itself. The wider geography around the Salton Sea could have also been included as a "control" variable of sorts, or at minimum to provide contrast to highlight how uniquely concerning the trends in compound exposure of extreme heat and dust and the resulting public health crisis at the Sea really is. The inclusion of tracts to the northwest near Beaumont, Riverside, and Redlands serves this function well, but a broader look at the Southern California region may have contributed useful information. The use of the 2014 SVI for SVI quartile stratification and overlays also presents its own limitations. While this SVI was selected due to fitting within the exact middle of the study period, using an updated SVI for 2026 (along with heat and dust data from the last several years) may have proven to be more useful for informing current policy, given that this would be more reflective of current conditions in the area. Finally, while correlation has been firmly demonstrated, it is ultimately hard to prove causation between the Salton Sea's shrinkage and the observed inequitable compound exposure trends and elevated asthma rates in the region based purely on this study alone. As stated previously, a higher resolution dataset and more in-depth statistical analysis with particle tracing from the exposed Salton Sea playa are needed to draw firmer conclusions on causal effects from the Sea's continued recession.

Future Work:

Conducting a follow-up study with more recent and pre-2003 QSA data could provide an updated and more holistic picture of the public health crisis at the Salton Sea over time. This would better inform state policymakers and task forces like the Salton Sea Management Program when proposing and implementing policy to mitigate compound exposure among the most vulnerable and disproportionately affected populations. Tracing dust PM 2.5 from the exposed Salton Sea playa to the surrounding region could help with establishing causal effects to bolster this, and presents the next logical avenue of research after this study. Such a study could provide compelling evidence of public health hazards directly resulting from the Salton Sea's decline and concurrently better inform water management and dust mitigation strategies moving forward. Directly linking these exposures to adverse public health outcomes like the asthma rates observed in this study would then also provide a strong impetus for these mitigation policies.

Investigating potential restoration and mitigation solutions is a natural follow-up after having established the worsening and inequitable compound exposure trends in the area. The Salton Sea Management Program has published regular portfolios of restoration solutions, and figures like Michael Cohen of the Pacific Institute think tank have exciting and innovative proposals for Salton Sea restoration and water management. Mr. Cohen has specifically advocated for a water optimization plan using a canal system combined with a geoengineered network of surrounding ponds to cover the exposed Salton Sea playa, serving the dual function of ecosystem restoration and dust mitigation (Management Program Staff, 2024). This plan is particularly compelling because it does not require the importation of additional sources of water from the already resource-constrained Southwestern United States, increasing project feasibility and long-term political viability (Management Program Staff, 2024). Other plans such as Jones et al.'s economic model for water leasing and importation from the local agricultural industry present clear solutions for restoring Sea extent, but are increasingly non-viable due to high quoted water pricing schemes that are far outside the Imperial Irrigation District's stated willingness to pay (Jones et al., 2025). Regardless, the demonstrated inequitable and concerning compound exposure trends at the Salton Sea represent profound issues of environmental justice and public health, and state and local government action in concert with outside innovators is warranted to ameliorate these effects as best as possible.

References

1. California Department of Water Resources Staff. “State and Local Agencies Complete New River Project in Calexico, Reaching Major Public Health Improvement Milestone.” *California Department of Water Resources*, State of California, 23 May 2025, water.ca.gov/News/News-Releases/2025/May-25/State-and-Local-Agencies-Complete-New-River-Project-in-Calexico.
2. Cantor, Alida, and Sarah Knuth. “Speculations on the Postnatural: Restoration, Accumulation, and Sacrifice at the Salton Sea.” *Environment and Planning A: Economy and Space*, vol. 51, no. 2, 2018, pp. 527–544, https://doi.org/10.1177/0308518x18796510.
3. CDC Staff. “Social Vulnerability Index.” *Centers for Disease Control and Prevention*, Centers for Disease Control and Prevention, 22 July 2024, www.atsdr.cdc.gov/place-health/php/svi/index.html.
4. Centers for Disease Control and Prevention/ Agency for Toxic Substances and Disease Registry/ Geospatial Research, Analysis, and Services Program. CDC/ATSDR Social Vulnerability Index 2018, 2016, 2014, 2010 Database California. https://www.atsdr.cdc.gov/placeandhealth/svi/data_documentation_download.html Accessed on 25 March 2026.
5. Evan, Amato T. “Downslope Winds and Dust Storms in the Salton Basin.” *Monthly Weather Review*, vol. 147, no. 7, 14 June 2019, pp. 2387–2402, https://doi.org/10.1175/mwr-d-18-0357.1.
6. Freund, Hannah, et al. “Microbiome Interactions and Their Ecological Implications at the Salton Sea.” *California Agriculture*, vol. 76, no. 1, 22 Apr. 2022, pp. 16–26, https://doi.org/10.3733/ca.2022a0002.
7. Johns Hopkins Bloomberg School of Public Health Staff. “Public Health Impacts of a Drying Saline Lake.” *Bloomberg American Health Initiative*, Johns Hopkins University, 2024, americanhealth.jhu.edu/sites/default/files/2024-11/JHU_2024_ExecSum_EarthJustice.pdf.
8. Johnston, Jill E., et al. “The Disappearing Salton Sea: A critical reflection on the emerging environmental threat of disappearing saline lakes and potential impacts on children’s health.” *Science of The Total Environment*, vol. 663, 1 May 2019, pp. 804–817, https://doi.org/10.1016/j.scitotenv.2019.01.365.
9. Jones, Benjamin A., et al. “Sending Agricultural Water to the Salton Sea to Improve Public Health? An Integrated Agri-Hydro-Health Economic Analysis.” *Journal of the Association of Environmental and Resource Economists*, 10 July 2025, https://doi.org/10.1086/737530.
10. Marlier, Miriam E., et al. “Compound Climate Exposures and Public Health: A Synthesis of Research and Future Directions.” *Annual Review of Public Health*, vol. 47, no. 1, 2 Apr. 2026, pp. 305–323, https://doi.org/10.1146/annurev-publhealth-090924-113926.

11. Popovich, Nadja, and Brad Plumer. "Who Has the Most Historical Responsibility for Climate Change." *The New York Times*, 12 Nov. 2021, https://www.nytimes.com/interactive/2021/11/12/climate/cop26-emissions-compensation.html. Accessed 18 May 2026.
12. PRISM Group Staff. *PRISM Group at Oregon State University*, Oregon State University, prism.oregonstate.edu/. Accessed 30 Apr. 2026.
13. Rahman, Md Mostafijur, et al. "The Effects of Coexposure to Extremes of Heat and Particulate Air Pollution on Mortality in California: Implications for Climate Change." *American Journal of Respiratory and Critical Care Medicine*, vol. 206, no. 9, 1 Nov. 2022, pp. 1117–1127, https://doi.org/10.1164/rccm.202204-0657oc.
14. Salton Sea Management Program Staff. "Salton Sea Long-Range Plan." *Salton Sea Management Program*, California Natural Resources Agency, Mar. 2024, saltonsea.ca.gov/wp-content/uploads/2024/03/Salton-Sea-Long-Range-Plan-Final-Mar-2024.pdf.
15. SimplyAnalytics Staff. *SimplyAnalytics*, SimplyAnalytics, simplyanalytics.com/. Accessed 30 Apr. 2026.
16. "TIGER/Line California State Shapefiles." *Index of /Geo/PVS/Tiger2010st/06_california/06*, United States Census Bureau, 3 Dec. 2010, www2.census.gov/geo/pvs/tiger2010st/06_California/06/.
17. UCSB Staff. "CHIRTS-Daily." *Climate Hazards Center UC Santa Barbara*, University of California, Santa Barbara, www.chc.ucsb.edu/data/chirtsdaily. Accessed 30 Apr. 2026.
18. Upadhyay, Ranjit Kumar, et al. "Restoration and Recovery of Damaged Eco-Epidemiological Systems: Application to the Salton Sea, California, USA." *Mathematical Biosciences*, vol. 242, no. 2, 2 Apr. 2013, pp. 172–187, https://doi.org/10.1016/j.mbs.2013.01.002.
19. Van Donkelaar, Aaron, et al. "North American Fine Particulate Matter Chemical Composition for 2000–2022 from Satellites, Models, and Monitors: The Changing Contribution of Wildfires." *ACS Publications*, vol. 1, no. 12, 11 Nov. 2024, pp. 1589–1600, https://doi.org/10.1021/acsestair.4c00151.
20. Zhang, Gengxi, et al. "Climate Change Determines Future Population Exposure to Summertime Compound Dry and Hot Events." Earth's Future, vol. 10, no. 11, 28 Oct. 2022, https://doi.org/10.1029/2022ef003015.